Relating the structural strength of concrete sewer pipes and material properties retrieved from core samples

Stanic, Nikola; Langeveld, Jeroen; Salet, Theo; Clemens, François

DOI
10.1080/15732479.2016.1187631

Publication date
2016

Document Version
Final published version

Published in
Structure and Infrastructure Engineering

Structure and Infrastructure Engineering

Maintenance, Management, Life-Cycle Design and Performance

ISSN: 1573-2479 (Print) 1744-8980 (Online) Journal homepage: http://www.tandfonline.com/loi/nsie20

Relating the structural strength of concrete sewer pipes and material properties retrieved from core samples

Nikola Stanić, Jeroen Langeveld, Theo Salet & François Clemens

To cite this article: Nikola Stanić, Jeroen Langeveld, Theo Salet & François Clemens (2017) Relating the structural strength of concrete sewer pipes and material properties retrieved from core samples, Structure and Infrastructure Engineering, 13:5, 637-651, DOI: 10.1080/15732479.2016.1187631

To link to this article: http://dx.doi.org/10.1080/15732479.2016.1187631

STRUCTURE AND INFRASTRUCTURE ENGINEERING, 2017
VOL. 13, NO. 5, 637–651
http://dx.doi.org/10.1080/15732479.2016.1187631

Taylor & Francis
Taylor & Francis Group

Relating the structural strength of concrete sewer pipes and material properties retrieved from core samples

Nikola Stanić[a], Jeroen Langeveld[a,b], Theo Salet[c,d] and François Clemens[a,e]

[a]Faculty of Civil Engineering and Geosciences, Water Management Department, Delft University of Technology, Delft, The Netherlands; [b]Partners4UrbanWater, Nijmegen, The Netherlands; [c]Witteveen + Bos Consulting Engineers, Deventer, The Netherlands; [d]Eindhoven University of Technology, Eindhoven, The Netherlands; [e]Deltares, Delft, The Netherlands

ABSTRACT
Drill core samples are taken in practice for an analysis of the material characteristics of concrete pipes in order to improve the quality of the decision-making on rehabilitation actions. Earlier research has demonstrated that core sampling is associated with a significant uncertainty. In this paper, the results of core samples are compared with the results of full-scale pipe cracking lab experiments. It is shown that the concrete of deteriorated sewer pipes shows a significant variability in material characteristics. Further it is shown that the formation of ettringite due to biochemical sulphuric corrosion is not necessarily limited to the crown of the pipe and also degradation of pipe material, measured by the carbonation depth, is occurring at the inside and outside of the pipe. It is concluded that tensile splitting strength and the carbonation depth are the two material property parameters of core sampling with a sufficiently high correlation ($R^2 > .90$) with the structural strength of the pipe. The thickness of the remaining 'healthy' concrete material is the optimal parameter, as this requires the smallest sampling size.

ARTICLE HISTORY
Received 13 August 2015
Revised 15 March 2016
Accepted 26 March 2016
Published online
9 February 2017

KEYWORDS
Collapse; concrete pipes; corrosion; degradation; sewers and drains; structural strength

1. Introduction

High-quality information on the actual status of the assets is a prerequisite for adequate sewer asset management. Currently, pipe age and visual sewer inspection are typically the primary sources of information used for decision-making for sewer rehabilitation (Halfawy, Dridi, & Baker, 2008). This practise is, however, not entirely in-line with the rehabilitation strategy defined in accordance to standard EN 752 (European Committee for Standardization, 2008). Dirksen et al. (2013) have shown that visual inspections are an unreliable source of information having a significant uncertainty. Additionally, visual inspection will not reveal invisible deterioration, like corrosion on the outside wall of a sewer (Aziz & Koe, 1990). As a result, it is not possible to derive the remaining strength of a sewer pipe using closed-circuit television camera (CCTV) inspection data.

The structural behaviour of buried concrete pipes is fairly well understood (e.g. Kang, Parker, & Yoo, 2007; Kim et al., 2010; Krizek & McQuade, 1978; Trautmann & O'Rourke, 1985), provided that information is available on the soil properties, pipe geometry and material properties. The pipe geometry, such as interior shape and related to this the estimated remaining wall thickness, can be measured by employing a laser-based profiler coupled to a CCTV (Clemens, Stanić, Van der Schoot, Langeveld, & Lepot, 2015; Duran, Althoefer, & Seneviratne, 2003). The material properties are typically measured by employing core sampling. Typically, a single core sample is taken from the crown of the sewer. However, Oualit, Jauberthie, Rendell, Melinge, and Abadlia (2012) and Stanić, de Haan, Tirion, Langeveld, and Clemens (2013) have demonstrated that material properties may vary with the location in the pipe at crown, invert and side positions and that core sampling is associated with significant uncertainties.

In the literature, some attempts to study the behaviour of buried pipes under laboratory conditions have been reported so far (Brachman, Moore, & Rowe, 2000; Trautmann & O'Rourke, 1985). However, to the knowledge of the authors no attempt to evaluate the structural response of deteriorated concrete sewer pipes under laboratory conditions has been reported. Furthermore, core samples can be exposed to a range of tests, ranging from general material properties such as density and water absorption to material strength properties, such as splitting tensile strength or crushing strength. It is unclear which material tests on core samples give the most representative results when compared with the 'real' structural strength of concrete sewer pipes.

In this article, the design of a laboratory set-up and experimental results for evaluating the performance of degraded sewer pipes is described. The test set-up is a simplification of actual field conditions in the sense that the pipe-ground interaction is not exactly in accordance with practise. The structural behaviour of these pipes was studied more in depth. A reliable prediction of

CONTACT Nikola Stanić N.Stanic@tudelft.nl

Table 1. Characteristics of studied sewer pipes.

No.	Origin	Service life	Surface damage class (BAF)	BAF class description
P01	De Hamer factory	New	–	
P08	The Hague	1924–2013	4	Missing aggregates or reinforcement outside the surface protrudes
P10	The Hague	1924–2013	4	
P02	Breda	1952–2013	3	Aggregates that protrude beyond the surface or visible reinforcement
P06	Breda	1952–2013	3	

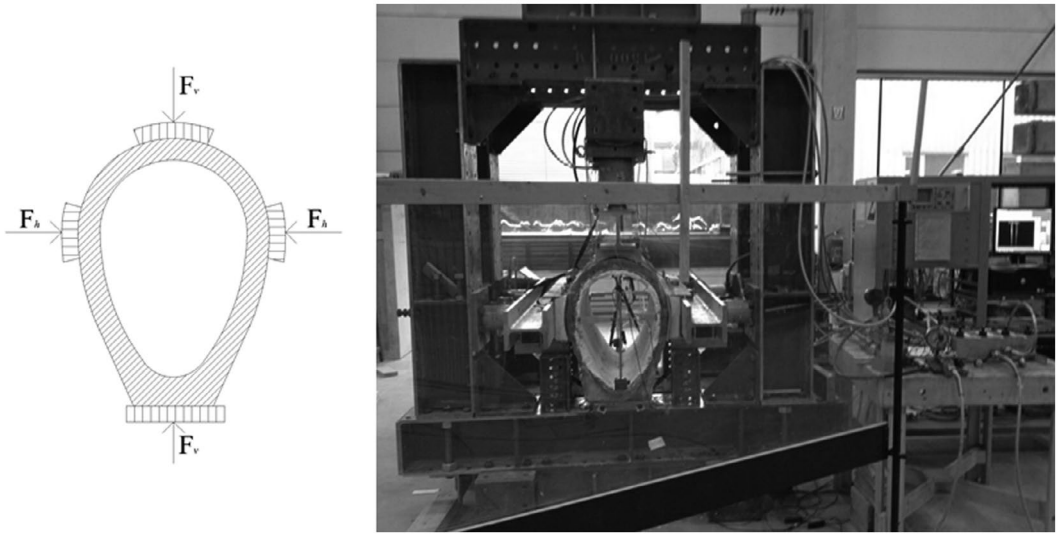

Figure 1. Schematic diagram of the adopted experiment principle (left) and actual experimental set-up (right).

the moment of pipe collapse (life cycle of the pipe) is critical for the optimisation of the inspection and maintenance of sewer structures. This is an important part of the assessment and rehabilitation strategy (see, European Committee for Standardization, 2008).

2. Materials and methods

The study was conducted on excavated sewer pipes that were scheduled for replacement according to the municipal sewer rehabilitation plans of The Hague and Breda. Prior to excavation visual inspections were performed to determine the condition of the inner surface of the sewer, i.e. surface damage by internal chemical (corrosion) or mechanical action (BAF). The registration of defects was done according to the visual inspection coding Standard EN 13508–2, while the Standard NEN 3399 was used to assign a level of severity to each defect – condition assessment (European Committee for Standardization, 2003; Nederlands Normalisatie-instituut, 2004a).

The pipes used in this project have been in service in combined sewer systems; they are egg-shaped with dimensions of 400/600 mm, 1-m long and made of concrete. The sewer in The Hague (P08 and P10) was located in a domestic housing area around old dunes. In this area the groundwater is below the sewer invert level (Gemeente Den Haag, 2011). The area in Breda (P02 and P06) used to be partly industrial and partly domestic. As a consequence, the Breda sewer was under a constant high traffic load for approximately 35 years. In this area, the groundwater is above the sewer crown level and the surrounding soil is a combination of peat, clay and sand (Oranjewoud, 2009). As a reference, a new concrete sewer pipe (P01) egg-shaped with dimensions of 400/600 mm, from De Hamer factory, was used to validate the experimental results. The new pipe was 2-m long, being shortened to .85 m length to allow testing in the same test facility. The quality and the shape of the new pipe meet the requirements required by the Netherlands and European standards NEN 7126, EN 1916 (European Committee for Standardization, 2002; Nederlands Normalisatie-instituut, 2004b). A detailed characteristic of each pipe is shown in Table 1.

2.1. Experimental set-up pipe structural strength

2.1.1. Boundary conditions

The first step considered in the design of the laboratory set-up involved simplification of boundary conditions experienced by an underground pipe. The structural performance of the pipe depends on both the soil and pipe stiffness and the resulting soil-structure interaction. A mechanical load on the pipes causes tensions having a vertical component F_v arising from the weight of the overlying materials above the pipe and a horizontal component F_h associated with the restraint against lateral soil movement within the embankment.

In the set-up design hypothetical soil properties were assumed (Young's modulus E = 80 MPa, Poisson's ratio ν = .25, angle of internal friction φ = 40°, angle of dilatancy $\psi = \varphi/4$, cohesion c = 0, and unit weight γ = 18 kN/m^3) (Brachman et al., 2000).

Figure 2. Test set-up used for four-point loading flexural tests.

Further, horizontal stresses are expressed as $K{\cdot}F_v$, where $K = \nu/(1-\nu) = .33$ is the coefficient of lateral earth pressure. This is a laboratory idealisation of field conditions. The applied experiment principle is shown in Figure 1 (left).

2.1.2. Test set-up design

The experimental set-up (Figure 1, right) consists of a test cell (steel frame/beams) and a concrete, egg-shaped sewer pipe. Applying a uniformly distributed pressure at the crown of the pipe may reasonably represent the vertical stress from the weight of the overburden material. As a reaction vertical stresses are present at the invert level of the pipe. Horizontal stresses could be simulated in a similar manner by applying lateral pressures equivalent to the horizontal stresses generated in the field. A system of oil pressure jacks and steel beams has been used to deliver stress on the pipe during the tests. In order to achieve a uniform distribution of stress, plaster moulds of pipe and soft boards were attached to the steel beams. The size of the load bearing plates is 1.5 times the pipe thickness. The tests were carried out at a loading rate of 10 kN/min. Sewer pipes were loaded in the set-up till the point of complete loss of carrying capacity and collapse of the pipe. Vertical and horizontal loads were measured together with their front and back vertical/horizontal displacements.

2.2. Pipe material testing methods

In order to determine the material properties of the pipes core sampling was applied. Core samples, however, provide information on the material properties of a few locations only (Stanić et al., 2013). Therefore, numerous samples (6 samples from the new pipe and 20 samples from each individual deteriorated pipes) were taken in order to gain data on the material properties of the whole pipe. According to standard EN 12390-1 the nominal size of the cylinder, i.e. height–diameter ration should be 2:1 (European Committee for Standardization, 2012). The nominal wall thickness (height) of the new pipe was ±70 mm. Consequently, this ration cannot be achieved in practise otherwise core diameter would be in the order of the maximum aggregate size (MAS), which is not according to standard ISO1920-6 (International Organization for Standardization, 2004). However, Neville (1995) noted that the height–diameter ration could be lower but not lower then 1; hence making the results unreliable. Consequently, drilled cylinders are also ±70 mm in order to keep height diameter ratio equal, which is a minimum test requirement. Furthermore, by visual inspection of the core samples MAS was estimated.

2.2.1. Compressive strength, density and water absorption

Compressive strength testing was conducted according to standards EN 12504-1, EN 12390-3 and EN 12390-7 (European Committee for Standardization, 2009a, 2009b, 2009e). If the core height diameter ratio was too small (caused by deterioration of the pipe) the real compressive strength was calculated according to CUR 74 (Civieltechnisch Centrum Uitvoering Research en Regelgeving, 2000). In some cases, no value is calculated because the height was too small and the ratio fell out of the scope of CUR 74. Before conducting compressive strength tests the samples were subjected to water absorption and a density test. Absorption tests are conducted according to EN 13369 (European Committee for Standardization, 2013). After completion of the water absorption tests the specimens were placed in a climate chamber for a few days (20 °C, Relative humidity 95%).

2.2.2. Splitting tensile strength and carbonation depth

Tests were conducted according to standards EN 12390-6 (European Committee for Standardization, 2009d). The test specimens used for the tensile strength were also used for the determination of the carbonation depth. For testing both, contact lengths were measured and the average length was used to calculate the splitting tensile strength. Further, carbonation depth was quantified on the leftover samples of the splitting tensile tests. Tests were conducted according to RILEM CPC-18 (1988) by spraying phenolphthalein and measuring the carbonation depth at two point in the section at the inner side and the outer side of the pipes. If the carbonation front was irregular another measurement point was taken.

2.2.3. Bending tensile strength

The four-point flexural tests (Figure 2) were carried out on rectangular samples (with dimension of 105 mm × 62–75 mm × 480 mm) taken from the upper and lower part of broken pieces of the pipes in order to quantify the ability of the concrete to resist deformation under load – EN 12390-5 (European Committee for Standardization, 2009c). The specimens were positioned in the middle of the rollers. In order to achieve a uniform distribution of stresses, steel plates and soft board roles are placed between roller and sample, if necessary with some plaster for correction. The four-point loading flexural tests were carried out at a loading rate of .5 mm/min. The bending (flexural) strength of both outer and inner side of the pipe was determined.

2.2.4. PFM microscopy

As Elsen (2006, p. 1421) has stated, 'PFM (Piezo Response Microscopy) is used as an important tool for diagnosing the degradation mechanism'. For the determination of the water cement ratio in the pipes optical fluorescence microscopy was used. For the test drill core samples from the invert and crown region of deteriorated pipes were taken (12 samples in total) to

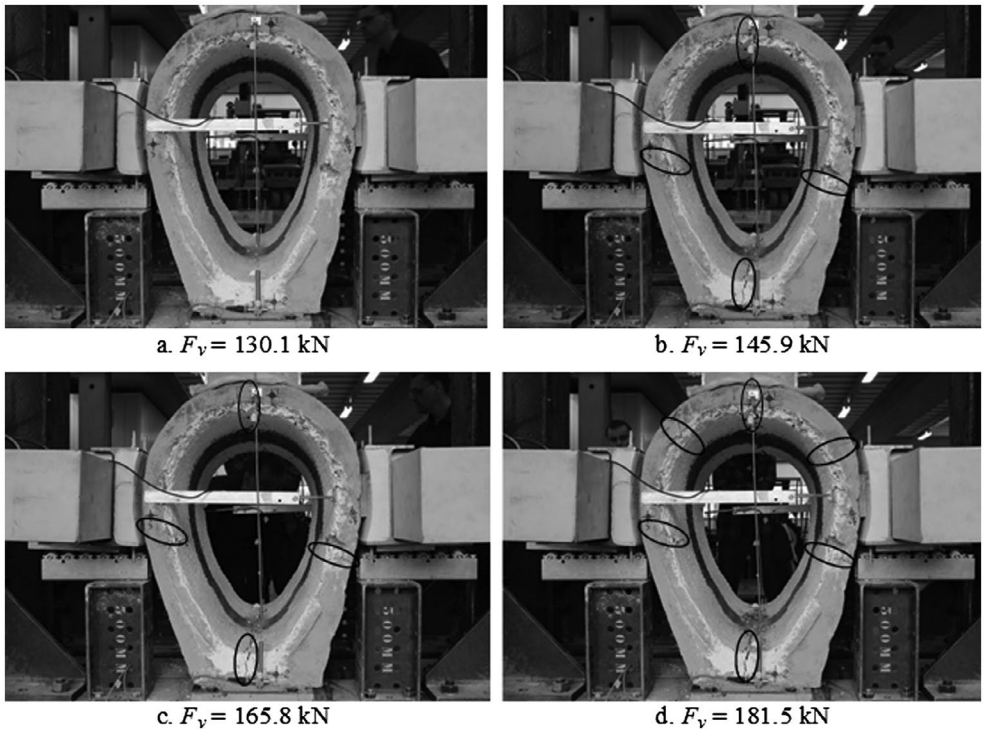

Figure 3. Successive stages in the test of a sewer pipe (P02) from Municipality of The Hague during the experiment.

make the thin sections. The specimens were vacuum impregnated which makes determination by fluorescence microscopy possible. When the samples are exposed to fluorescence light all voids, pores and cracks become highlighted. The brightness of the sample gives indication of the porosity and thereby the water to cement ratio. This brightness was compared with reference samples with a known water to cement ratio.

3. Results and discussion

3.1. Pipe structural strength

For all pipes, cracks appeared at the same location suggesting that the distribution of stresses through the pipes during the tests was the same. The first crack always appeared at the pipe invert level, followed by cracks at the pipe crown area and one on each side (Figure 3).

Figure 4 shows load-displacement response for the studied pipes. The results show clearly the regions of crack formation and points of the pipe collapse. Major cracks on the new pipe appeared at the vertical load, F_v = 280 kN. The major cracks on the 61- and 89-year-old pipes appeared at around 25 and around 55% smaller load (Figure 4). With an increase in the load, however, the pipes resisted collapse due to the combination of vertical and horizontal loads.

Test results showed that the complete loss of carrying capacity for the new pipe was at 330 kN. Also, results showed that the 61-year-old pipes could withstand almost the same amount of load, F_v = 315 kN and F_v = 290 kN. In contrast, the 89-year-old pipes could withstand a load up to 185 kN and 162 kN (around 40% less stress). This implies that pipes, which are considered old (61-year old), can withstand similar loads as a new pipe before total collapse takes place. Furthermore, from the results it can be seen that the first cracks occurred with displacement of about .6 mm, and that the pipes reach the point of collapse with displacements between 13 and 19 mm.

The test method for the crushing strength of new concrete pipes is defined by standards NEN 7126 and EN 1916 (European Committee for Standardization, 2002; Nederlands Normalisatie-instituut, 2004b). For egg-shaped pipes with a flat base, the uniaxial load shall be applied through one top bearer and they shall be supported on two bottom bearers placed with their centres at a distance equal to .3 times the internal diameter or width. De Hamer concrete factory performs these quality check test regularly and they get an average value of 131 kN/m (σ = 1.87 kN/m) for the pipe crushing strength. This crushing strength is about 60% smaller than the experimental set-up recorded crushing strength. This result was to be expected, as the horizontal support in the experiments has a strong impact on the strength of the pipe/soil construction. The results of the quality check test should be regarded only as the material quality check for the whole pipe and not as the pipe crushing strength.

3.2. Pipe material testing methods

The results of the splitting tensile strength, density and water absorption test show that the difference between measured values (maximum and minimum) increases with worsening of conditions, being the highest for the cores from the Municipality of The Hague. However, the results of compressive strength test do not show this trend. This is probably due to the effect of MAS. MAS for the pipes P02 and P06 was 16 mm, and for P08 and P10 was 32 mm. The relative strength values of cores gradually decreased with the increase in maximum size of the aggregate. This becomes more apparent for the smaller diameter cores (<100 mm), which is in this case (Tuncan, Arioz, Ramyar, & Karasu, 2008). The ratio

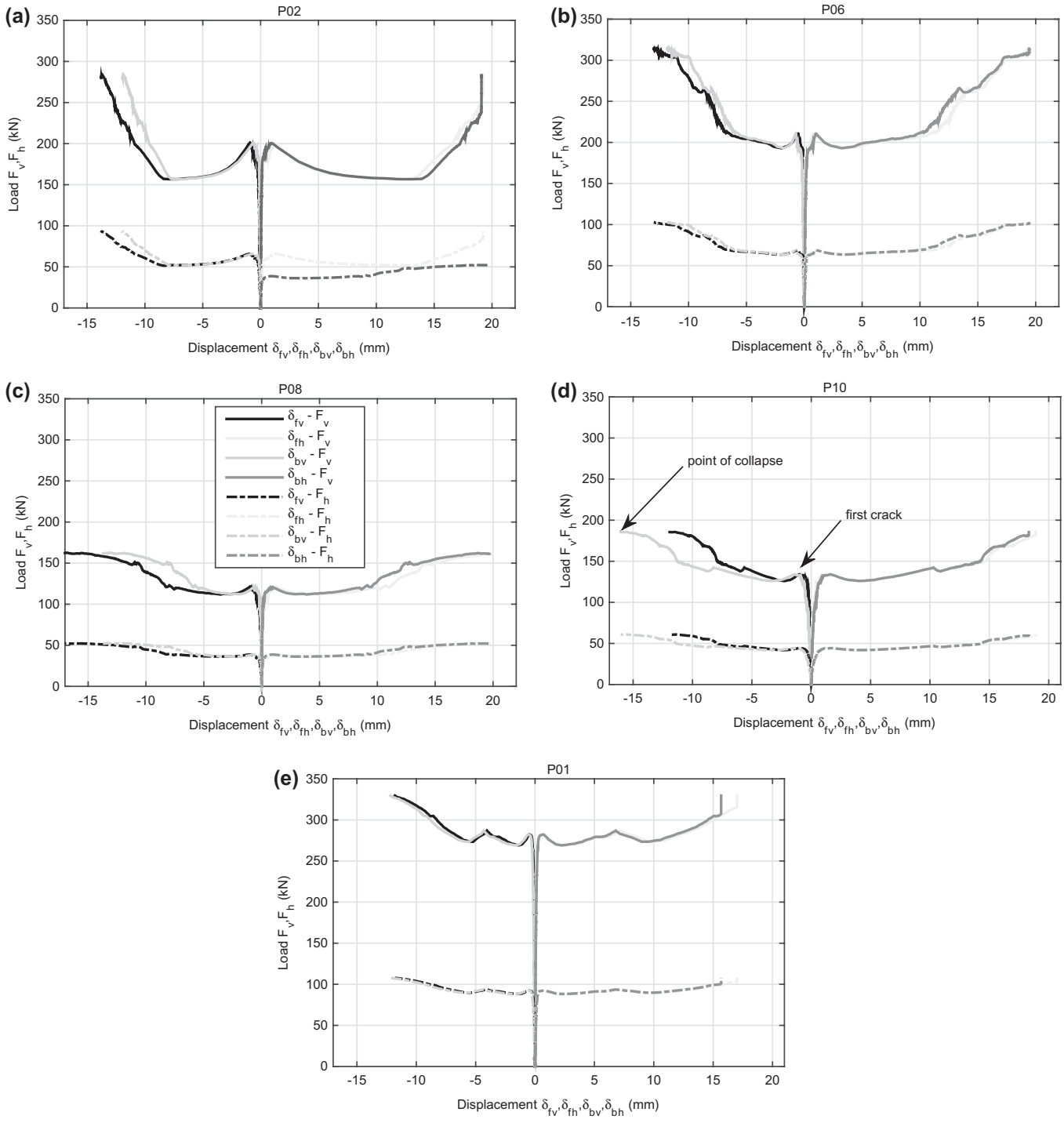

Figure 4. Force-displacement response for; (a,b) the 61-year-old sewer pipes - P02, P06; (c,d) the 89-year-old sewer pipes - P08, P10; (e) the new sewer pipe - P01. Legend: F_v – vertical force; F_h – horizontal force; δ_{fv} – front vertical displacement; δ_{fh} – front horizontal displacement; δ_{bv} – back vertical displacement; δ_{bh} – back horizontal displacement.

of core diameter to the MAS should generally be greater than 3 (International Organization for Standardization, 2004). This was fulfilled for the pipes P01, P02 and P06. However, this was not fulfilled for the cores from the pipes P08 and P10.

The results of the material tests are compared with the pipe structural strength in the next section. This section describes in some detail the results of the carbonation depth and the four-point flexural tests.

Concrete carbonation occurs when Ca bearing phases present are attacked by CO_2 from air and/or from water, and converted to $CaCO_3$. Figures 5 and 6 show box plots for the carbonation depth for the outside and the inside of drill core samples for the old pipes. As can be seen, there is large variability. The ranges for the crown and the lateral locations are almost equal, while the carbonation depth at the inside invert location is significantly less than at the crown and the lateral locations. This was to be expected and points at the occurrence of the classic process crown deterioration (see, e.g. O'Connell, McNally, and Richardson (2010)). On the other hand, chemical attack from the outside was also occurring and is almost

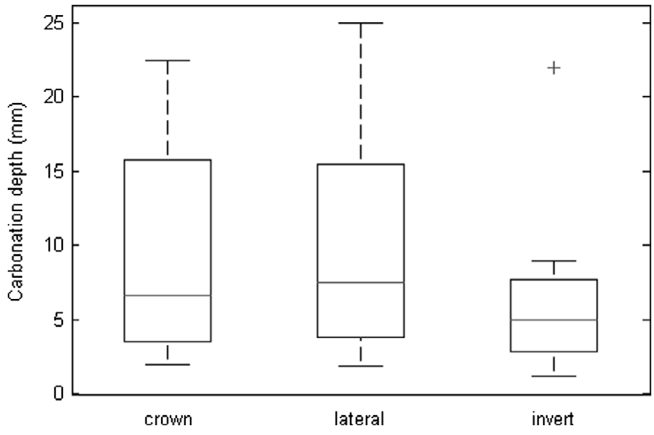

Figure 5. Boxplot for the carbonation depths at the inside for pipes P02, P06, P08 and P10; discriminating between crown, lateral and invert positions. On each box, the central mark is the median, the edges of the box are the 25th and 75th percentiles, the whiskers extend to the most extreme data points not considered outliers (approximately ± 2.7σ), and outliers are plotted individually.

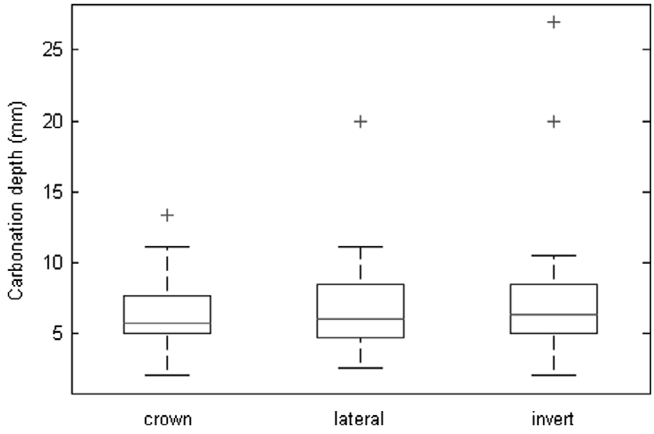

Figure 6. Boxplot for the carbonation depths at the outside for pipes P02, P06, P08 and P10; discriminating between crown, lateral and invert regions. On each box, the central mark is the median, the edges of the box are the 25th and 75th percentiles, the whiskers extend to the most extreme data points not considered outliers (approximately ± 2.7σ), and outliers are plotted individually.

identical for all three regions (Figure 6). Soil surrounding pipes was probably acidic thus attacking concrete and in combination with acidic groundwater (in case of Breda, pipes P02 and P06) (Hobbs, 2001). Although the (bio-)chemical attack at the outside caused less damage than at the inside, the material deterioration is considerable, thus confirming the relevance of outside damage (Oualit et al., 2012).

The four-point flexural tests were carried out on rectangular samples (with dimension of 105 mm × 62–75 mm × 480 mm) taken from the upper and lower part of broken pieces of the pipes. Results show a high variability between samples per individual pipe and between samples between pipes (Figure 7). The variability may be partly due to the fact that the tested beams were not completely rectangular due to the shape of the pipes. In addition to the irregular-shaped beams, the 61 and 89 old pipes apparently did not deteriorate uniformly over the pipe length and circumference. Furthermore, the initial quality of the concrete is most likely not the same for the studied sewer pipes. However, this cannot be tested as there is no recorded information on the initial quality of the studied old concrete sewer pipes.

PFM experimental results showed that concrete of all pipes is too porous, therefore it was not possible to determine the relevant material property of water to cement ratio. Furthermore, along the Interfacial Transition Zone, the concrete was porous (Figure 8). At the surface of the thin section some very small vertical cracks were observed.

Generally deterioration in concrete sewer pipes only occurs at the inside due to biological produced acid (see, e.g. Bielecki & Schremmer, 1987; Pomeroy & Parkhurst, 1977). Biogenic sulphide acid attack is a microbiologically induced type of corrosion. Indirectly from the bacterial decomposition of sewage H_2S gas forms. The gas rises and combines with oxygen and with moisture condensed on upper surfaces of the sewer pipe to form H_2SO_4 acid that attacks concrete (see, e.g. Hammerton, 1944). Sulphuric acid reacts with the calcium hydroxide and the calcium silicate hydrate gel in concrete to form gypsum (see, e.g. Attigobe & Rizkalla, 1988). In the second stage of the corrosion of concrete, gypsum could go through another cycle of reactions, eventually producing ettringite and/or thaumasite.

In addition, sulphuric acid can cause both dissolution and swelling of concrete (Soutsos, 2010). Furthermore, in literature there are cases described that show that sulphur related corrosion does occur due to other mechanisms (see e.g. Oualit et al. (2012)). For the pipes P02, P06, P08 and P10 the presence of ettringite, an indication of sulphate attack, was investigated using PFM. Ettringite was found in all samples (Figure 9). When looking at the sections with polarised light, over the whole thin section samples (from top and bottom) large amounts of ettringite were found; however no large cracks were detected. Furthermore, the very small cracks, which can be seen under fluorescent light, were not observed under polarised light. Therefore, no link can be found between the amounts of ettringite and presence the small cracks.

The formation of ettringite in hardened concrete in relation to concrete deterioration is the result of complex long-term processes in which the concrete composition, technological factors during concrete production and the effects of the surroundings are important (Stark & Bollmann, 1999). Moreover, the pipes from Municipalities of Breda and The Hague (P02, P06, P08 and P10, respectively) were produced *in situ* and installed. In conclusion, they were made in a non-controlled environment and using water of unknown quality (possible presence of sulphate) which could also explain the presence of ettringite in the concrete. As Stark and Bollmann (1999, p. 21) have stated: 'It cannot be excluded that ettringite is often not involved in the damage mechanism and thus only a consequence of the microstructure damage caused by other processes'.

There is no clear division in damaged or undamaged parts of the concrete. Visually some colouring and deterioration were observed, but overall there is no real deterioration (cracks or loss of coherence) visible under the microscope. This means there is no damaged layer present and therefore no thickness of the possibly damaged layer can be determined. PFM experimental results could therefore not clearly distinguish the degradation mechanism. However, it can be concluded that material degradation of the sewer pipes from both Breda and The Hague occurred in the same manner, although the pipes originate from different environments with respect to soil properties and groundwater levels.

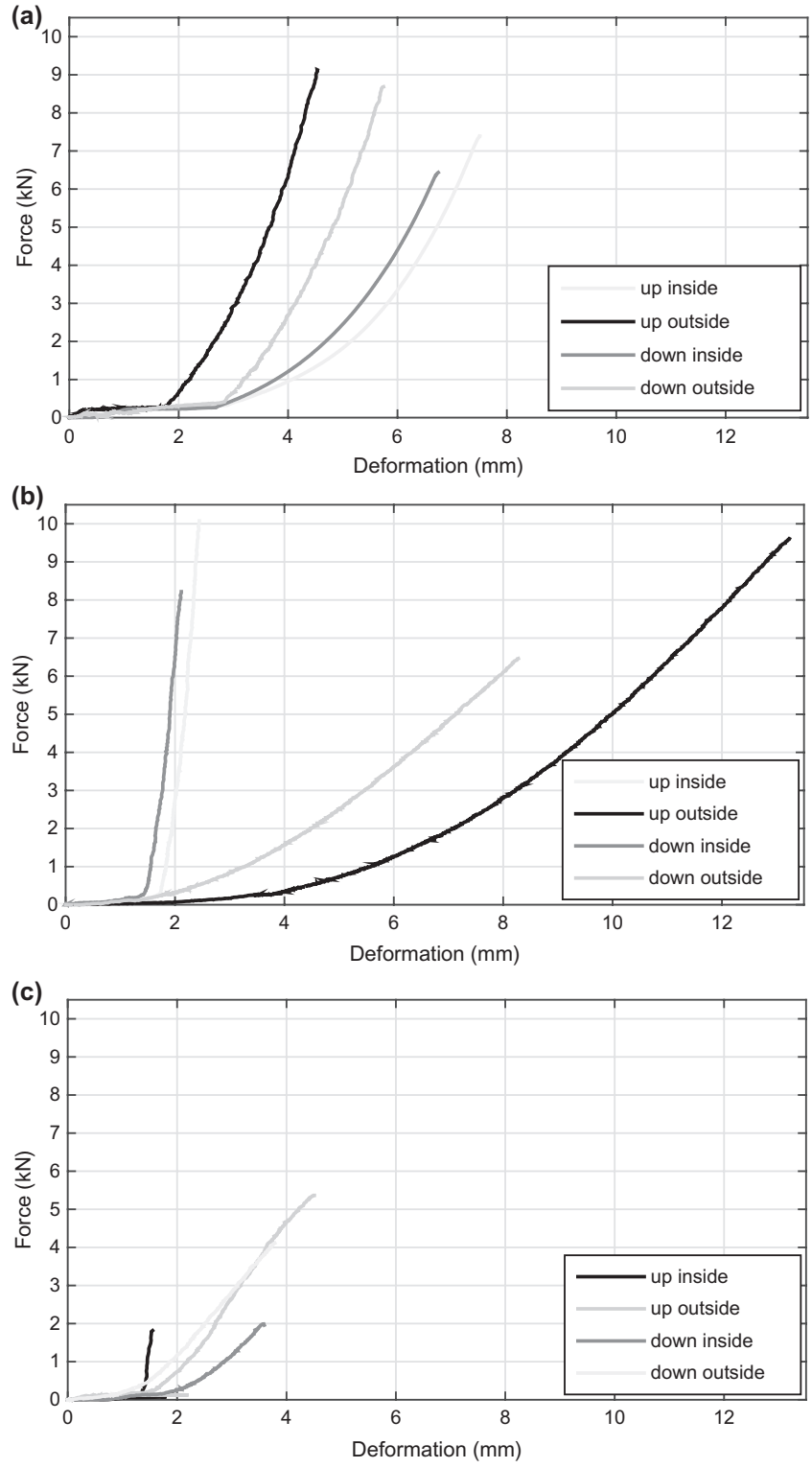

Figure 7. The four-pint flexural test force-deformation response for; (a) the new sewer pipe – P01; (b) the 60-year-old sewer pipe – P02; (c) the 90-year-old sewer pipe – P08.

3.3. Relation between material properties and structural strength

The relation between the data obtained from the sample tests and the force applied ($F_{v,max}$) on the pipes at the moment the first crack appeared in the pipe crack experiments are shown in Figures 10–17. In the graphs a distinction is made between minimal, maximum and mean values of the materials properties per pipe, from these graphs the following observations are made:

- With respect to carbonation depth, the sum of the inner and outer carbonation show a better correlation with $F_{v,max}$ than the values obtained for the inside wall alone. Further, it can be seen that the mean values (R^2 = .98)

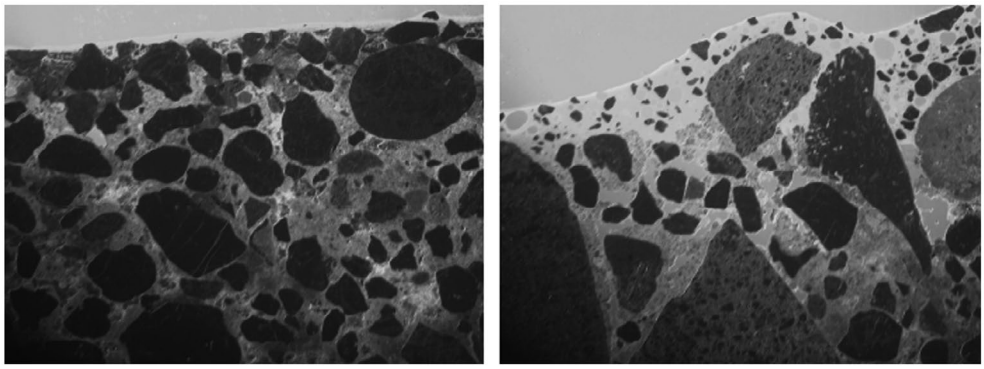

Figure 8. Examples of the studied thin section under the fluorescence light (P02 and P06).

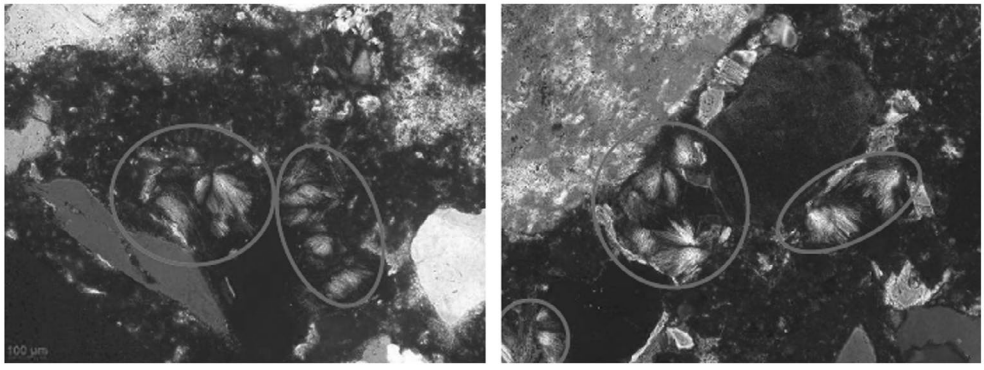

Figure 9. Examples of the studied thin sections under the polarised light with the highlighted ettringite (P06 and P02).

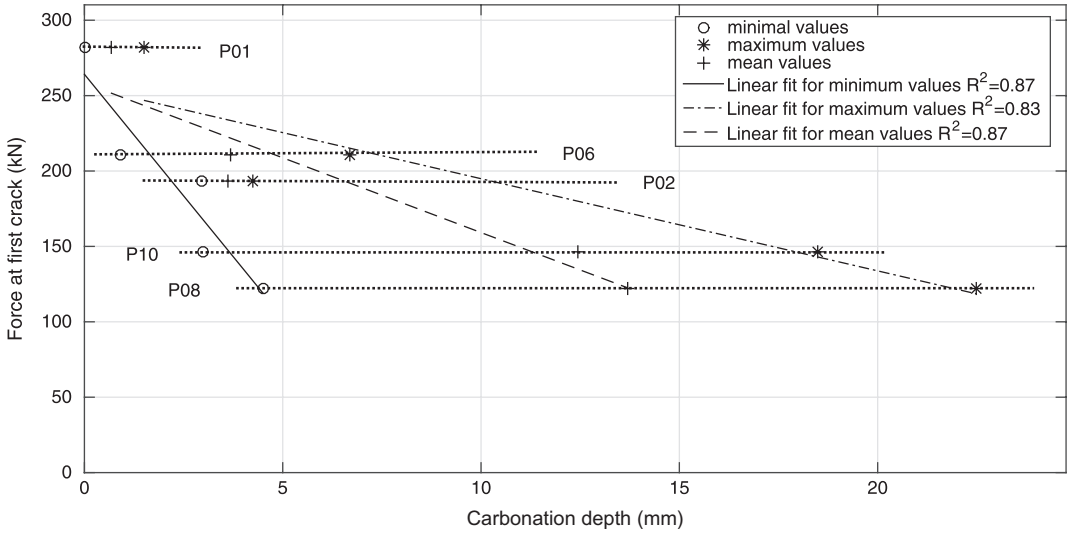

Figure 10. Relation between force at the first crack and carbonation depth at the inner wall of the pipes.

correlate slightly better with $F_{v,max}$ than the maximum values observed (R^2 = .92). (Figure 10 and 11). With respect to carbonation depth, the mean value is therefore the most appropriate parameter.

- With tensile splitting (Figure 12), the best correlation with $F_{v,max}$ is obtained for the minimum values found for the tensile splitting strength with an R^2 of .96. The correlation with the mean splitting tensile strength, with an R^2 of .83 is still acceptable.
- With respect to tensile bending strength (Figure 13), the values for the tensile bending strength show very low correlations for the minimum, mean and maximum. Tensile bending strength is therefore not a very suitable parameter to assess the material properties.

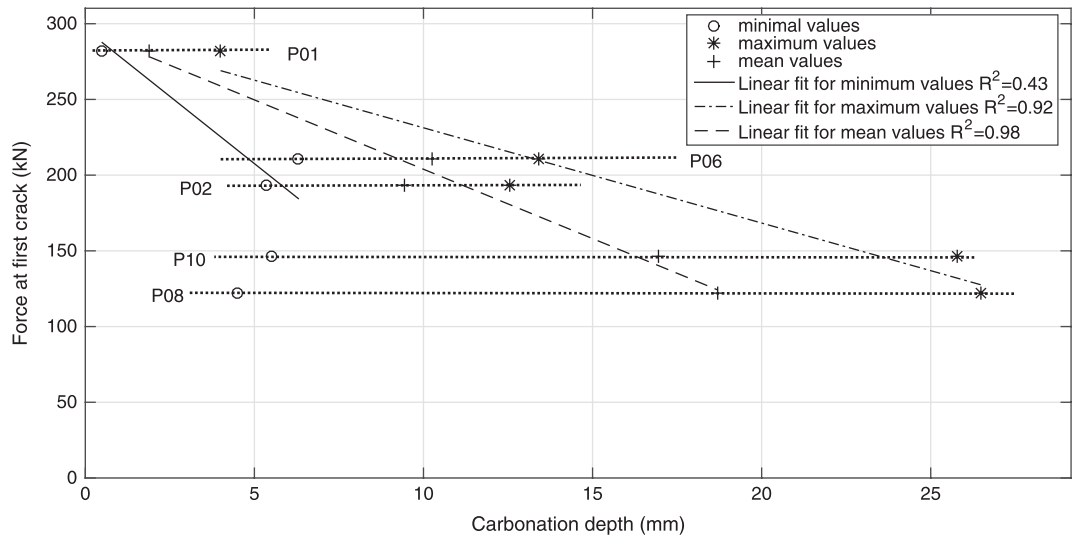

Figure 11. Relation between force at the first crack and the carbonation depth at the inside and outside wall of the pipes.

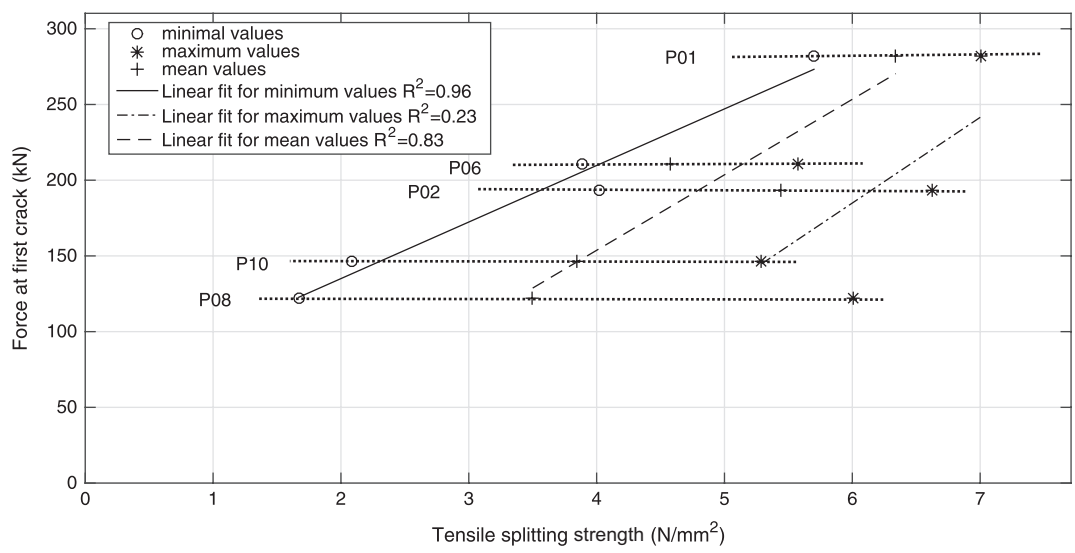

Figure 12. Relation between force at the first crack and the tensile splitting strength.

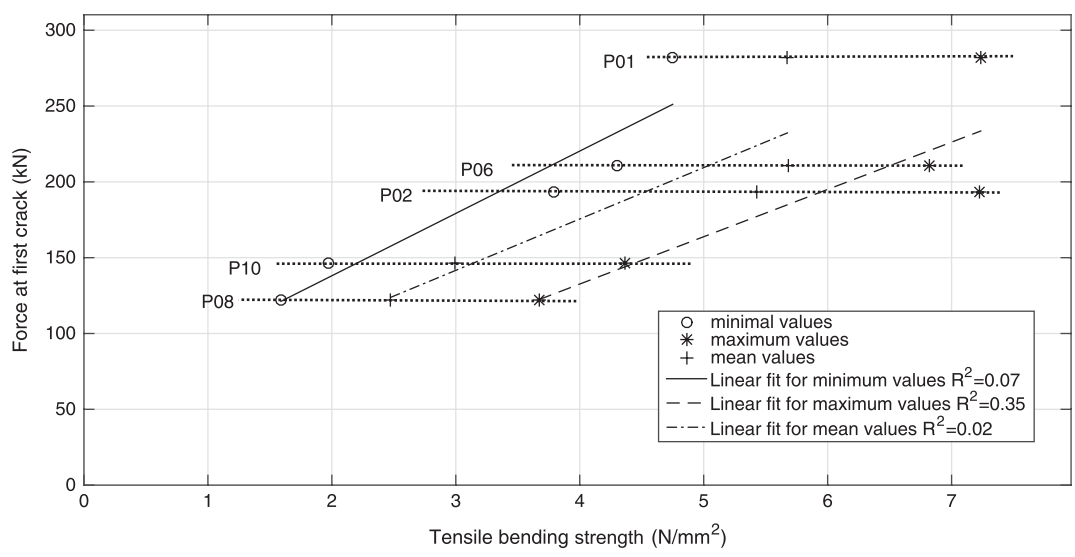

Figure 13. Relation between force at the first crack and the tensile bending strength.

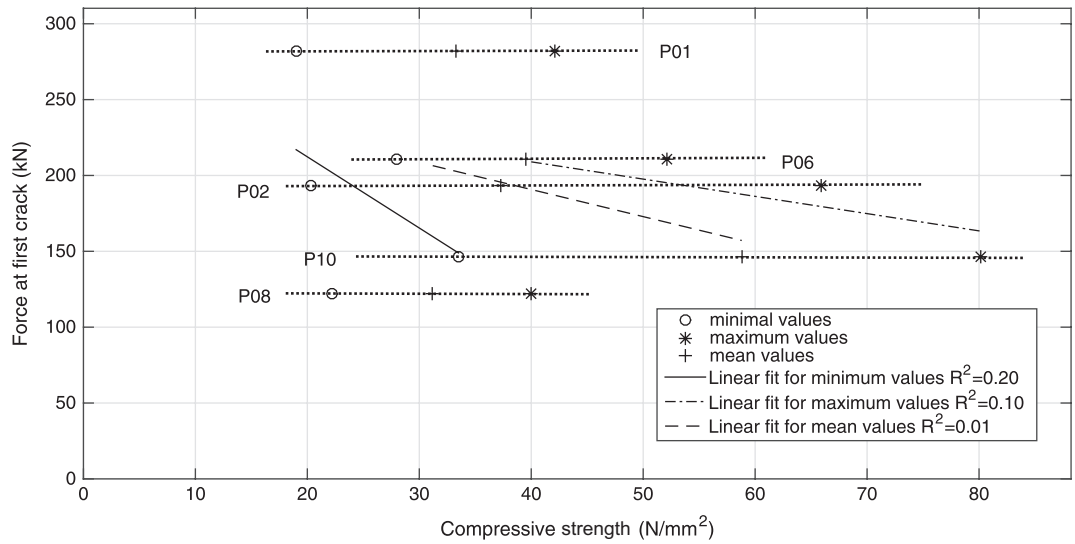

Figure 14. Relation between force at the first crack and the compressive strength.

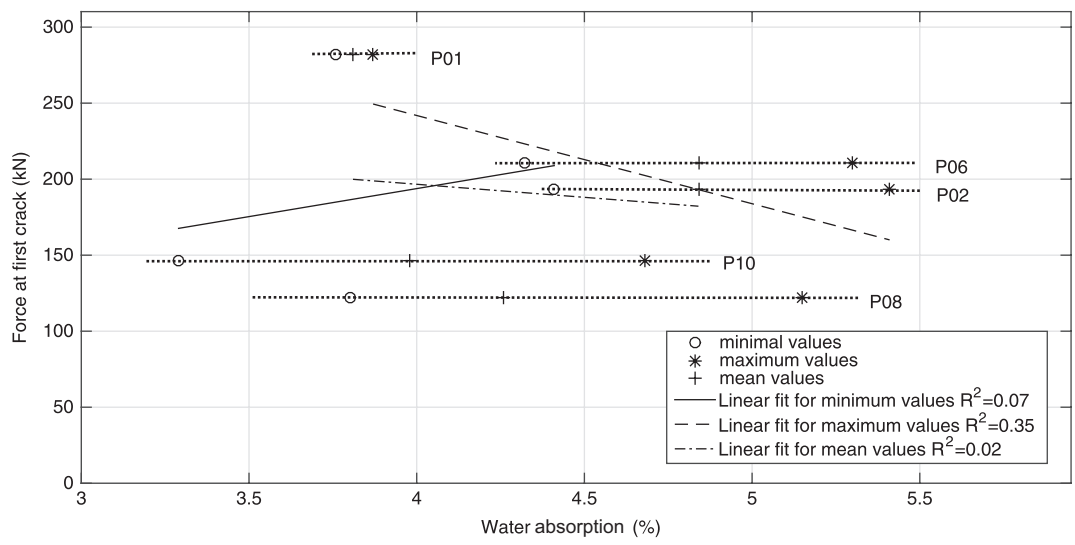

Figure 15. Relation between force at the first crack and the water absorption.

- Compressive strength seems to have no significant with $F_{v,max}$ (Figure 14) and is therefore also not a suitable parameter to assess pipe strength.
- The material properties water absorption and density (Figures 15 and 16) show only a significant correlation (R^2 = .89) for the minimum values found for the material density, with respect to water absorption only a very weak correlation (R^2 = .35) between the maximum values and $F_{v,max}$ was found.

The minimal tensile splitting strength apparently gives the best information with respect to the material's properties, while the carbonation depth gives the best information with respect to the geometry. The latter is illustrated when the remaining thickness of the healthy material is taken as a parameter. The thickness of the healthy material is defined by the measured wall thickness minus the values found for the carbonation depth on the inside and outside of the pipe. Figure 17 shows the results. Indeed, the mean and maximum values of the remaining healthy material have, respectively, a R^2 of .90 and .93 with the force applied when the first crack appeared.

It should be noted that carbonation is a relevant degradation mechanism in reinforced concrete, as this reduces the protection of the reinforcement from corrosion. For non-reinforced concrete, the impact of carbonation on the quality of the concrete is less unambiguous. Taylor (1997) showed that carbonation has both positive and negative effects on concrete. It results in a decrease in porosity thus making the non-reinforced concrete carbonated paste stronger. On the other hand, Jerga (2004) notes that carbonation can lead to shrinkage of concrete.

Research of Atis (2003, 2004) shows that there is a strong relation between carbonation and compressive strength of concrete, as well as between carbonation and porosity. Strength decreases and the porosity increases with the increase in carbonation depth. In addition, experimental results of the pipes described in this paper allowed the study of the relation between the carbonation depth and the structural strength, i.e. bending tensile strength (see, Table 2). The two samples were taken for four-point loading flexural tests from the upper and lower part of each pipe in order to determine the bending tensile strength on the inside and outside of each pipe. Results showed that the

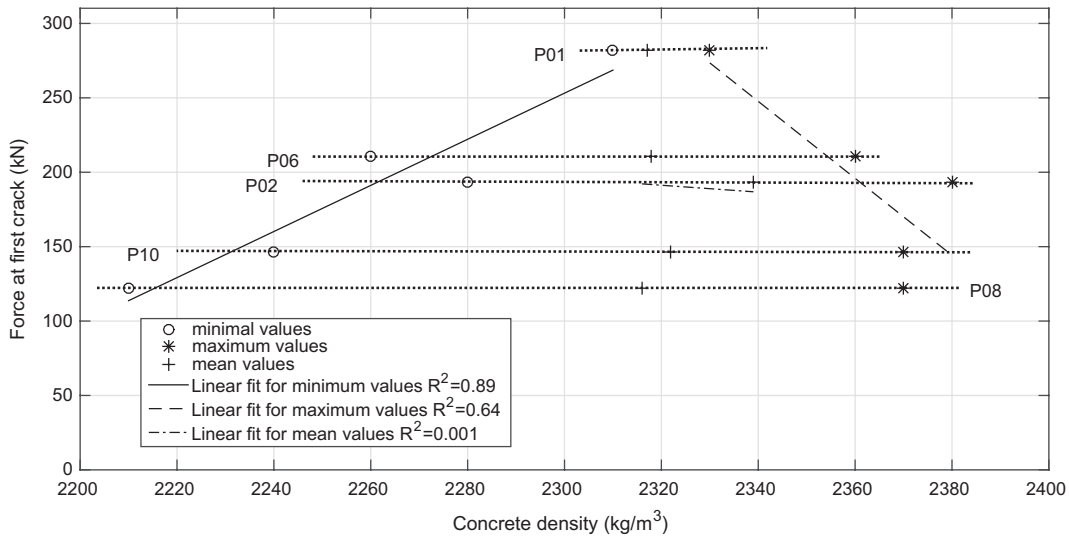

Figure 16. Relation between force at the first crack and the density of the concrete.

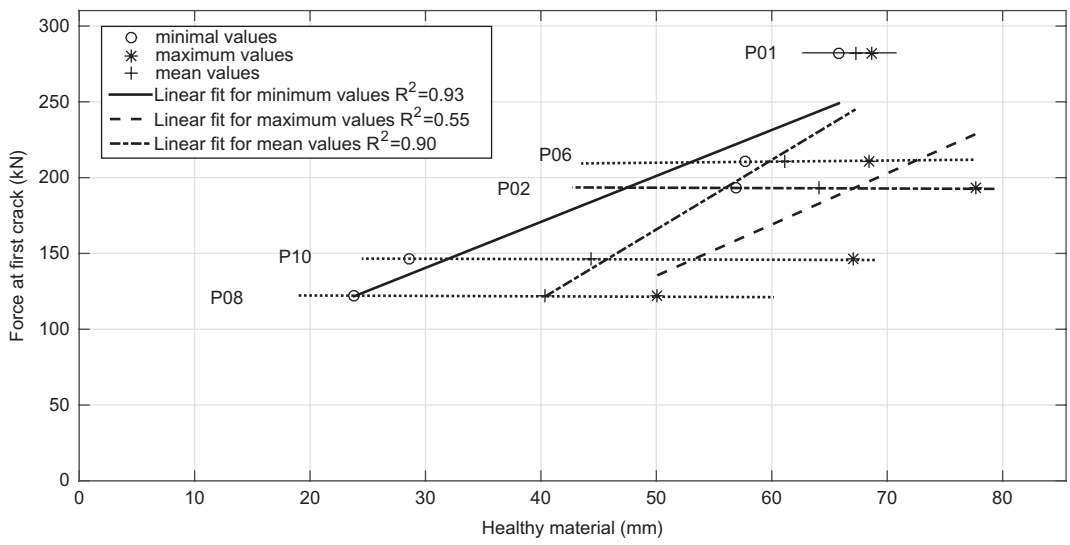

Figure 17. Relation between thickness of the remaining healthy material and force at the first crack.

Table 2. Relation between carbonation depth and bending tensile strength.

	Upper (crown) region		Lower (invert) region	
Sample	Stressed from inside σ_f (N/mm^2)	Stressed from outside [cd (mm)]	Stressed from inside σ_f (N/mm^2)	Stressed from outside [cd (mm)]
P02	5.25 [6.10]	7.22 [3.28]	3.79 [6.18]	5.46 [3.86]
P06	6.41 [7.44]	6.82 [4.63]	5.20 [5.74]	4.30 [2.68]
P08	3.67 [2.38]	1.59 [15.45]	2.82 [8.77]	1.81 [10.33]
P10	4.36 [1.88]	1.97 [14.12]	3.48 [2.90]	2.15 [6.00]

Legend: σ_f – bending strength, cd – mean carbonation depth in the stressed region.

samples under stress lost their structural integrity easier when the samples were more affected by carbonation; hence demonstrating the relation between the increase in carbonation depth and decrease in bending tensile strength. The relation was more obvious for the 89-year-old pipes (P08 and P10).

Overall, it seems that carbonation and its impact on materials and constructive properties of concrete sewer pipes is not restricted to reinforced concrete. Therefore, the authors feel that future research into this impact would be in place. In this paper, the term 'healthy material' is regarded as the material that is not affected by the degradation process(es).

Furthermore, it is observed that the material characteristics of the new pipe (P01) are more homogeneous than of the old pipes for most parameters, apart from compressive strength and tensile bending strength. It is also these two parameters that show the least correlation with the force at the appearance of the first crack. Apparently, the homogeneity of the material decreases with age and, as a consequence, the number of samples required increases

Table 3. Calculated sample size required for 95% reliability.

Pipe	Parameter	Initial estimate for the mean value	Initial estimate for the standard deviation	Sample size for the mean values. Based on Equation (2)
New	Remaining healthy material	67.3 mm	2.1 mm	1
	Density	2317.0 kg/m^2	11.5 kg/m^3	1
	Tensile splitting strength	6.34 N/mm^2	.86 N/mm^2	7
P02	Remaining healthy material	64.0 mm	5.4 mm	3
	Density	2339.0 kg/m^3	2846.0 kg/m^3	1
	Tensile splitting strength	5.44 N/mm^2	.90 N/mm^2	11
P06	Remaining healthy material	61.0 mm	3.4 mm	2
	Density	2318.0 kg/m^3	30.5 kg/m^3	1
	Tensile splitting strength	4.58 N/mm^2	.53 N/mm^2	6
P08	Remaining healthy material	40.3 mm	8.9 mm	19
	Density	2316.0 kg/m^3	43.3 kg/m^2	1
	Tensile splitting strength	3.50 N/mm^2	1.32 N/mm^2	55
P10	Remaining healthy material	44.3 mm	11.0 mm	24
	Density	2322.0 kg/m^3	41.0 kg/m^3	1
	Tensile splitting strength	3.85 N/mm^2	2.08 N/mm^2	112

for older, more deteriorated, pipes, which has significant consequences for the reliability of core sampling. This conclusion was drawn although it is well known that the initial quality of the concrete for all tested pipe was not the same. The conclusion is based on the approach that concrete (in a similar environment) over the long period of time has tendency to deteriorate in the same manner.

Due to the inability to access independent samples to do rigorous cross-validation, PRESS-related statistics were used. Holiday, Ballard, and McKeown (1995) recommended the use of the PRESS approach for cross-validation of regression models when having small data-sets, as well as a means of dealing with the problems of data-splitting. This is a method based on the jackknife technique. The idea is to fit the model without the ith observation x_i and use this fitted model to predict the response $\hat{y}_{(i)}$, at x_i. The PRESS residuals are defined as $e_{(i)} = y_i - \hat{y}_{(i)}$. The process is repeated for all n observations. The PRESS statistic is computed as:

$$\text{PRESS} = \sum_{i=1}^{n} e_{(i)}^2 \tag{1}$$

Once determined, the PRESS statistic was used to calculate a predicted R^2 (R^2_{PRESS}) using the following formula: $R^2_{\text{PRESS}} = 1 - (\text{PRESS}/\text{TSS})$, where TSS it the total sum of squares for the original regression equation (Myers, 1990). The smaller the difference between the two values for coefficient of determination, the more stable the model for prediction. For the given R^2 values the best R^2 predictions (R^2_{PRESS}) were obtained for the minimal tensile splitting strength ($R^2_{\text{PRESS}} = .92$) and for the mean carbonation depth ($R^2_{\text{PRESS}} = .96$). Differences in values are small, i.e. a decrease in .04 and .02 from R^2 for their prediction model, respectively. Overall, these models appear to be stable, hence they can be regarded as representative.

3.4. Sampling strategies for core sampling

For older concrete pipes, a rather large variability in the material characteristics result from the analyses. Furthermore, it was shown that the relation between material characteristics and pipe failure strength is relatively strong for maximum and mean values of carbonation depth ($R^2 = .92$ and $R^2 = .98$), minimum values for density ($R^2 = .89$) and minimum values of tensile splitting strength ($R^2 = .96$). This implies that when deciding on the number of samples to be analysed this variability has to be taken into account.

Assuming a normal distribution and using the experimental results as a first estimate for the mean and the standard deviation, the following calculations can be made for the estimate of the sample size as a function of the reliability; with respect to the mean, the sampling size can be estimated by Louangrath (2014):

$$n \geq \left[\frac{Z_{\alpha/2} s}{E}\right]^2 \tag{2}$$

where E is the allowed difference between the estimated mean value and the 'true' value and $z_{\alpha/2}$ defines the reliability interval (e.g. $\alpha = .05$ defines the 95% confidence interval).
With $\alpha = .05$, E is 10% of the initial estimated mean value for carbonation depth and tensile splitting strength and $E = 5\%$ for density, formula (2) shows that for new pipes one core sample is sufficient to estimate the remaining thickness of healthy material, but at least seven samples are needed to determine the tensile splitting strength (see, Table 3). For older pipes, with lower initial mean values and higher standard deviations, the number of samples for the thickness of healthy material ranges between 2 and 24 samples and for tensile splitting strength between 11 and 112 samples (see, Table 3).

Especially, with respect to the parameter tensile splitting strength, for which the minimum value is more relevant than the mean value, the number of samples to be taken is also defined with the certainty with which the variance of the parameter has to be known. The confidence interval for the variance σ^2 is given by:

$$\frac{(n-1)s^2}{\chi^{2\ (\alpha/2)}_{n-1}} \leq \sigma^2 \leq \frac{(n-1)s^2}{\chi^{2\ (1-\alpha/2)}_{n-1}} \tag{3}$$

in which $\frac{(n-1)s^2}{\chi^{2(\beta)}_{n-1}}$ is the β quantile for chi-squared distribution with $n-1$ degrees of freedom, n is the sample size, s is the estimate for the standard deviation. If the interval is set to a certain minimal acceptable length; γs^2 then the sampling size is defined by:

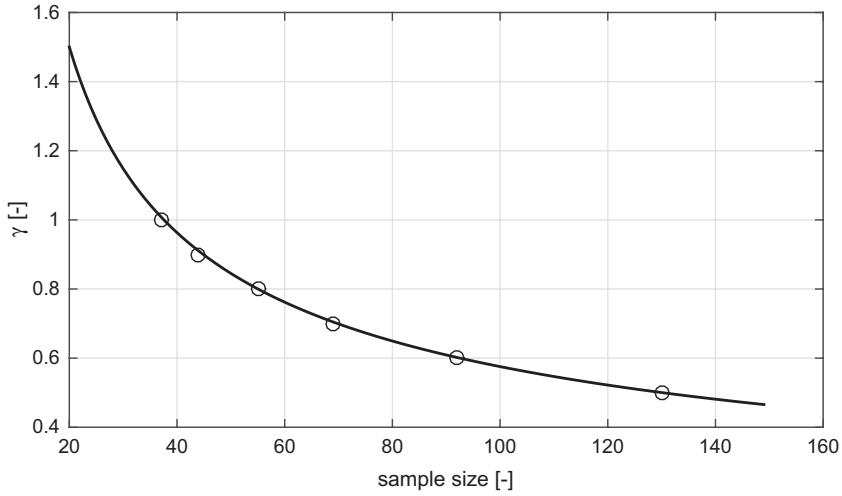

Figure 18. Relation between relative confidence interval and sample size.

$$\left(\frac{(n-1)s^2}{\chi^{2\ (\alpha/2)}_{n-1}} - \frac{(n-1)s^2}{\chi^{2\ (1-\alpha/2)}_{n-1}}\right) < \gamma s^2 \rightarrow \left(\frac{(n-1)}{\chi^{2\ (\alpha/2)}_{n-1}} - \frac{(n-1)}{\chi^{2\ (1-\alpha/2)}_{n-1}}\right) < \gamma \quad (4)$$

Figure 18 depicts the relation between the sampling size and the relative confidence interval γ for σ^2, as can be seen that in order to obtain a value for γ smaller than .5, a sample size of at least 131 has to be chosen. Even for $\gamma = 1$, the sample size should be at least 38.

It is clear that, in order to obtain reliable data, a number of samples have to be taken and that this number is highly variable. For instance, the pipes P02 and P06 on one hand and P08 and P10 were located in the same stretch of sewer and show significant different results. From the pipes analysed in this study the number of samples to be taken seem to increase with age (new = 0 years of service, P02 and P06 have seen 61 year of service, P08 and P10 have seen 89 years of service). The number of samples indicated is prohibitive in two ways: costs and the fact that after taking that many samples, the conclusion would be 'The operation was success full, a pity the patient died'. As a consequence, the parameter remaining healthy concrete material is clearly to be preferred over the parameter tensile splitting strength.

4. Conclusions and outlook

Sewer systems deteriorate due to ageing, overloading, misuse and mismanagement. The challenge for sewer asset management is to be able to estimate a safety margin for the collapse of pipes. Further, the presence of cracks does not imply that the pipe collapses. Cracked pipes could still withstand a reasonable additional load. Different factors, like road conditions, traffic load and especially local soil conditions may influence the sewer's lifespan. It is disputable to regard pipe age and CCTV as main and sufficient information sources in deciding upon sewer system renewal.

Core sampling is a destructive technique that is generally accepted for determining the material properties of concrete sewer pipes. The results show that concrete deteriorates non-uniformly in space and time; while deviations between results increases with worsening of conditions of studied pipe. Due to somewhat ambiguous nature of carbonation and its impact on materials and constructive properties of (non-reinforced) concrete sewer pipes further research is suggested. In addition, PFM experimental results show that it is difficult to distinguish the degradation mechanism, due to the influence of numerous factors starting from the production stage to the end of pipe service life. Furthermore, based on the comparison of the results of controlled lab pipe cracking experiments and core sampling results of the pipe material, the following conclusions can be drawn:

- The minimal tensile splitting strength gives the best information with respect to the material's properties.
- The mean carbonation depth (i.e. loss of 'healthy' wall thickness) gives the best information with respect to the geometry.
- For severely deteriorated pipes the required number of core samples increases to a prohibitively high level. For these very deteriorated pipes, other non-destructive techniques should be developed as an alternative.

For sewer rehabilitation decisions, it is necessary to be able to calculate the remaining strength of the soil-pipe construction environment for deteriorated pipes. Further research will concentrate on simulations with a Finite Element Method, with the pipe geometry information provided by a laser profiling and material properties by core sampling. The lab test set-up presented in this manuscript is a simplification of actual field conditions and can be used to verify a finite element model (e.g. DIANA). Such a model will be able to accurately predict the structural behaviour of a sewer pipe; thus the structural behaviour of these pipes will be studied in more depth. Furthermore, the effects of the different soil properties and/or conditions can be studied as well as the effects of different kinds of loads (e.g. traffic load) on the structural response. The final model can be used to determine the remaining load bearing capacity of a sewer pipe and to determine the type of information needed to further enhance the decision-making process.

Acknowledgements

The authors would like to acknowledge the funding by (in alphabetical order) ARCADIS, Deltares, Gemeente Almere, Gemeente Breda, Gemeente 's-Gravenhage, Gemeentewerken Rotterdam, Gemeente Utrecht, GMB Rioleringstechniek, Grontmij, KWR Watercycle Research Institute, Royal Haskoning DHV, Stichting RIONED, STOWA, Tauw, vanderValk + deGroot, Waterboard De Dommel, Waternet and Witteveen + Bos as part of the Urban Drainage Research program. A special acknowledgement is for the staff of the Municipality of The Hague, the Municipality of Breda and for the staff of the structure laboratory of TU Eindhoven for their assistance with the experimental set-up and giving access to their facilities.

Disclosure statement

No potential conflict of interest was reported by the authors.

Funding

ARCADIS, Deltares, Gemeente Almere, Gemeente Breda, Gemeente 's-Gravenhage, Gemeentewerken Rotterdam, Gemeente Utrecht, GMB Rioleringstechniek, Grontmij, KWR Watercycle Research Institute, Royal HaskoningDHV, Stichting RIONED, STOWA, Tauw, vanderValk + deGroot, Waterboard De Dommel, Waternet and Witteveen + Bos as part of the Urban Drainage Research program.

References

Atiş, C. D. (2003). Accelerated carbonation and testing of concrete made with fly ash. *Construction and Building Materials, 17*, 147–152.

Atiş, C. D. (2004). Carbonation-porosity-strength model for fly ash concrete. *Journal of Materials in Civil Engineering, 16*, 91–94.

Attigobe, E. K., & Rizkalla, S. H. (1988). Response of concrete to sulfuric acid. *ACI Material Journal, 85*, 481–488.

Aziz, M., & Koe, L. (1990). Durability of concrete sewers in aggressive sub-soils and groundwater conditions. In *Geotechnical Aspects of Restoration Works on Infrastructures and Monuments*, edited by A. S. Balasubramaniam, 299–310, Rotterdam: Balkema.

Bielecki, R., & Schremmer, H. (1987). *Biogene Schwefelsäure-Korrosion in teilgefüllten Abwasserkanälen* [Biogene sulfuric acid corrosion in partially filled sewers]. Braunschweig: Leichtweiβ-Institut.

Brachman, R. W., Moore, I., & Rowe, R. (2000). The design of a laboratory facility for evaluating the structural response of small-diameter buried pipes. *Canadian Geotechnical Journal, 37*, 281–295.

Civieltechnisch Centrum Uitvoering Research en Regelgeving. (2000). *Onderzoek aan de betonconstructie* [Research on the concrete structure]. (CUR 74). Gouda: CUR.

Clemens, F. H. L. R., Stanić, N., Van der Schoot, W., Langeveld, J. G., & Lepot, M. (2015). Uncertainties associated with laser profiling of concrete sewer pipes for the quantification of the interior geometry. *Structure and Infrastructure Engineering, 11*, 1218–1239. doi: http://dx.doi.org/10.1080/15732479.2014.945466

Den Haag, G. (2011). *Gemeentelijk Rioleringsplan Den Haag 2011–2015: Goed riool, gezonde leefomgeving* [Municipal sewer plan hague 2011–2015: Good sewer, healthy environment]. The Hague: Municipality of The Hague.

Dirksen, J., Clemens, F. H. L. R., Korving, H., Cherqui, F., Le Gauffre, P., Ertl, T., Plihal, H., Müller, K., & Snaterse, C. T. M. (2013). The consistency of visual sewer inspection data. *Structure and Infrastructure Engineering, 9*, 214–228. doi:http://dx.doi.org/10.1080/15732479.2010.541265

Duran, O., Althoefer, K., & Seneviratne, L. D. (2003). Pipe inspection using a laser-based transducer and automated analysis techniques. *IEEE/ASME Transactions on Mechatronics, 8*, 401–409.

Elsen, J. (2006). Microscopy of historic mortars – A review. *Cement and Concrete Research, 36*, 1416–1424.

European Committee for Standardization. (2002). *Concrete pipes and fittings, unreinforced, steel fibre and reinforced*. (EN 1916). Brussels: CEN.

European Committee for Standardization. (2003). *Investigation and assessment of drain and sewer systems outside buildings – Part 2: Visual inspection coding system*. (EN 13508-2). Brussels: CEN.

European Committee for Standardization. (2008). *Drain and sewer systems outside buildings*. (EN 752). Brussels: CEN.

European Committee for Standardization. (2009a). *Testing concrete in structures – Part 1: Cored specimens – Taking, examining and testing in compression*. (EN 12504-1). Brussels: CEN.

European Committee for Standardization. (2009b). *Testing hardened concrete – Part 3: Compressive strength of test specimens*. (EN 12390-3). Brussels: CEN.

European Committee for Standardization. (2009c). *Testing hardened concrete – Part 5: Flexural strength of test specimens*. (EN 12390-5). Brussels: CEN.

European Committee for Standardization. (2009d). *Testing hardened concrete – Part 6: Tensile splitting strength of test specimens*. (EN 12390-6). Brussels, CEN.

European Committee for Standardization. (2009e). *Testing hardened concrete – Part 7: Density of hardened concrete*. (EN 12390-7). Brussels: CEN.

European Committee for Standardization. (2012). *Testing hardened concrete – Part 1: Shape, dimensions and other requirements for specimens and moulds*. (EN 12390-1). Brussels: CEN.

European Committee for Standardization. (2013). *Common rules for precast Concrete products* (EN 13369). Brussels: CEN.

Halfawy, M. R., Dridi, L., & Baker, S. (2008). Integrated decision support system for optimal renewal planning of sewer networks. *Journal of Computing in Civil Engineering, 22*, 360–372.

Hammerton, C. (1944). The corrosion of cement and concrete. *The Surveyor*, p. 587.

Hobbs, D. (2001). Concrete deterioration: Causes, diagnosis, and minimising risk. *International Materials Reviews, 46*, 117–144.

Holiday, D. B., Ballard, J. E., & McKeown, B. C. (1995). PRESS-related statistics: Regression tools for cross-validation and case diagnostics. *Medicine and Science in Sports and Exercise, 27*, 612–620.

International Organization for Standardization. (2004). *Testing of concrete – Part 6: Sampling, preparing and testing of concrete cores*. Geneva: ISO.

Jerga, J. (2004). Physico-mechanical properties of carbonated concrete. *Construction and Building Materials, 18*, 645–652.

Kang, J., Parker, F., & Yoo, C. H. (2007). Soil-structure interaction and imperfect trench installations for deeply buried concrete pipes. *Journal of Geotechnical and Geoenvironmental Engineering, 133*, 277–285.

Kim, J., O'Connor, S., Nadukuru, S., Lynch, J. P., Michalowski, R., Green, R. A., ... Bradshaw, A. (2010). *Behavior of full-scale concrete segmented pipelines under permanent ground displacements.* Paper presented at the SPIE Health Monitoring of Structural and Biological Systems, San Diego, CA.

Krizek, R. J., & McQuade, P. V. (1978). Behavior of buried concrete pipe. *Journal of Geotechnical and Geoenvironmental Engineering, 104*, 815–836. (ASCE 13899 Proceeding).

Louangrath, P. T. (2014). *Sample size determination for non-finite population.* Paper presented at the International Conference on Discrete Mathematics and Applied Science, Bangkok, Thailand.

Myers, R. (1990). *Classical and modern regression with applications* (2nd ed.). Boston, MA: Duxbury Press.

Nederlands Normalisatie-instituut. (2004a). *Buitenriolering – Classificatiesy steem bij visuele inspectie van objecten* [Sewerage systems outside buildings – Classification system for visual inspection of objects]. (NEN 3399). Delft: NEN.

Nederlands Normalisatie-instituut. (2004b). *Buizen en hulpstukken van ongewapend, gewapend en staalvezelbeton* (Concrete pipes and fittings, unreinforced, steel fibre and reinforced). (NEN 7126). Delft: NEN.

Neville, A. M. (1995). *Properties of concrete* (4th ed.). Harlow: Longman Group.

O'Connell, M., McNally, C., & Richardson, M. G. (2010). Biochemical attack on concrete in wastewater applications: A state of the art review. *Cement and Concrete Composites, 32*, 479–485.

Oranjewoud. (2009). *Bemalingsadvies: Wooneilanden Talmazone en riolering Talmastraat Breda* [Land drainage advice: Residential islands talma zone and sewer talmastraat breda]. (189027). Breda: Author.

Oualit, M., Jauberthie, R., Rendell, F., Melinge, Y., & Abadlia, M. (2012). External corrosion to concrete sewers: A case study. *Urban Water Journal, 9*, 429–434.

Pomeroy, R., & Parkhurst, J. (1977). Forecasting of sulfide buildup rates in sewers. *Progress in Water Technology, 9*, 621–628.

RILEM. (1988). CPC-18 measurement of hardened concrete carbonation depth. *Materials and Structures, 21*, 453–455.

Soutsos, M. (2010). *Concrete durability: A practical guide to the design of durable concrete structures*. London: Thomas Telford.

Stanić, N., de Haan, C., Tirion, M., Langeveld, J. G., & Clemens, F. H. L. R. (2013). Comparison of core sampling and visual inspection for assessment of concrete sewer pipe condition. *Water Science & Technology, 67*, 2458–2466.

Stark, J., & Bollmann, K. (1999). *Delayed ettringite formation in concrete*. Paper presented at the Nordic Concrete Research Meeting, Oslo, Norway.

Taylor, H. F. W. (1997). *Cement chemistry* (2nd ed.). London: Thomas Telford.

Trautmann, C. H., & O'Rourke, T. D. (1985). Lateral force-displacement response of buried pipe. *Journal of Geotechnical Engineering, 111*, 1077–1092.

Tuncan, M., Arioz, O., Ramyar, K., & Karasu, B. (2008). Assessing concrete strength by means of small diameter cores. *Construction and Building Materials, 22*, 981–988.